

# Modulation of Rac Localization and Function by Dynamin

Günther Schlunck,<sup>\*†</sup> Hanna Damke,<sup>‡</sup> William B. Kiosses,<sup>\*</sup> Nicole Rusk,<sup>§</sup>  
Marc H. Symons,<sup>§</sup> Clare M. Waterman-Storer,<sup>‡</sup> Sandra L. Schmid,<sup>‡</sup> and  
Martin Alexander Schwartz<sup>\*||¶</sup>

<sup>\*</sup>Division of Vascular Biology, <sup>‡</sup>Department of Cell Biology, The Scripps Research Institute, La Jolla, California 92037; and <sup>||</sup>Center for Oncology and Cell Biology, North Shore-Long Island Jewish Research Institute, Manhasset, New York 11030

Submitted January 17, 2003; Revised September 3, 2003; Accepted September 8, 2003

Monitoring Editor: Anne Ridley


The GTPase dynamin controls a variety of endocytic pathways, participates in the formation of phagosomes, podosomal adhesions, and invadopodia, and in regulation of the cytoskeleton and apoptosis. Rac, a member of the Rho family of small GTPases, controls formation of lamellipodia and focal complexes, which are critical in cell migration and phagocytosis. We now show that disruption of dynamin<sup>-2</sup> function alters Rac localization and inhibits cell spreading and lamellipodia formation even though Rac is activated. Dominant-negative K44A dynamin<sup>-2</sup> inhibited cell spreading and lamellipodia formation on fibronectin without blocking cell adhesion; dynamin<sup>-2</sup> depletion by specific small interfering RNA inhibited lamellipodia in a similar manner. Dyn2(K44A) induced Rac mislocalization away from cell edges, into abnormal dorsal ruffles, and led to increased total Rac activity. Fluorescence resonance energy transfer imaging of Rac activity confirmed its predominant localization to aberrant dorsal ruffles in the presence of dominant-negative dyn2(K44A). Dyn2(K44A) induced the accumulation of tubulated structures bearing membrane-bound Rac-GFP. Constitutively active but not wild-type GFP-Rac was found on macropinosomes and Rac-dependent, platelet-derived growth factor-induced macropinocytosis was abolished by Dyn2(K44A) expression. These data suggest an indispensable role of dynamin in Rac trafficking to allow for lamellipodia formation and cell spreading.

## INTRODUCTION

Endocytosis, actin polymerization, and intracellular signal transduction are intimately coupled (reviewed in Ceresa and Schmid, 2000; Di Fiore and De Camilli, 2001). The endocytic uptake of plasma membrane receptors may serve to switch off receptor signaling by ligand dissociation in endosomes and receptor degradation in lysosomes. Endocytosis and subsequent membrane trafficking are also essential to position signaling molecules in specific subcellular compartments, allowing for spatio-temporal regulation of downstream signaling pathways. Finally, endocytosis is needed to recycle membrane proteins in rapid demand, for example, in neuronal signaling and cell migration.

Dynamin is a 96-kDa GTPase that was initially thought to function mainly in the receptor-mediated internalization of clathrin-coated vesicles (van der Bliek *et al.*, 1993; Damke *et al.*, 1994) but is now known to control clathrin-independent uptake of caveolae (Henley *et al.*, 1998; Oh *et al.*, 1998; Pelkmans *et al.*, 2002) and noncaveolar lipid rafts as well (Lamaze *et al.*, 2001). Dynamin is generally thought to mediate the detachment of nascent vesicles from the plasma membrane. Three different mammalian dynamin isoforms have been described: neuronal dynamin-1, ubiquitously expressed dynamin-2, and dynamin-3, which is found in testes, lung, and brain. Increasing evidence implicates dynamin in a range of membrane trafficking and signaling functions (reviewed in Schmid *et al.*, 1998; McNiven *et al.*, 2000a). Dominant-negative dynamin can interfere with mitogen-activated protein kinase activation (Kranenburg *et al.*, 1999; Hislop *et al.*, 2001). Overexpression of WT dynamin-2 is able to induce apoptosis (Fish *et al.*, 2000) and its interactions with the cytoskeleton influence the movement of intracellular vesicles (Lee and De Camilli, 2002; Orth *et al.*, 2002), modulate cell shape (McNiven *et al.*, 2000b), affect podosomal adhesions (Ochoa *et al.*, 2000; Lee and De Camilli, 2002), invadopodia (Baldassarre *et al.*, 2003), and phagocytosis (Gold *et al.*, 1999). In growth factor-stimulated cells, dynamin localizes to lamellipodia and their derivatives, dorsal membrane ruffles (Cao *et al.*, 1998). Most recently, dynamin was shown to form a cytoskeleton-regulatory complex with cortactin and Arp2/3 (Schafer *et al.*, 2002) that has a role in actin reorganization after growth factor stimulation (Krueger *et al.*, 2003). Specific functions for dynamin in

Article published online ahead of print. Mol.Biol.Cell 10.1091/mbc.E03-01-0019. Article and publication date are available at [www.molbiolcell.org/cgi/doi/10.1091/mbc.E03-01-0019](http://www.molbiolcell.org/cgi/doi/10.1091/mbc.E03-01-0019).

 Online version of this article has video material for some figures. Online version is available at [www.molbiolcell.org](http://www.molbiolcell.org).

Present addresses <sup>||</sup>Departments of Microbiology and Biomedical Engineering, Cardiovascular Research Center, University of Virginia, Charlottesville, VA 22908; and <sup>¶</sup>University Eye Hospital, Division of Experimental Ophthalmology, Josef-Schneider Strasse 11, D-97080 Würzburg, Germany.

<sup>¶</sup> Corresponding author. E-mail: [maschwartz@virginia.edu](mailto:maschwartz@virginia.edu).

Abbreviations used: FN, fibronectin; FRET, fluorescence resonance energy transfer; GFP, green fluorescent protein; GST, glutathione S-transferase; HRP, horseradish peroxidase; PBD, p21-binding domain of PAK1; PDGF, platelet-derived growth factor; PRD, proline-, arginine-rich domain; siRNA, small interfering RNA; WT, wild type.

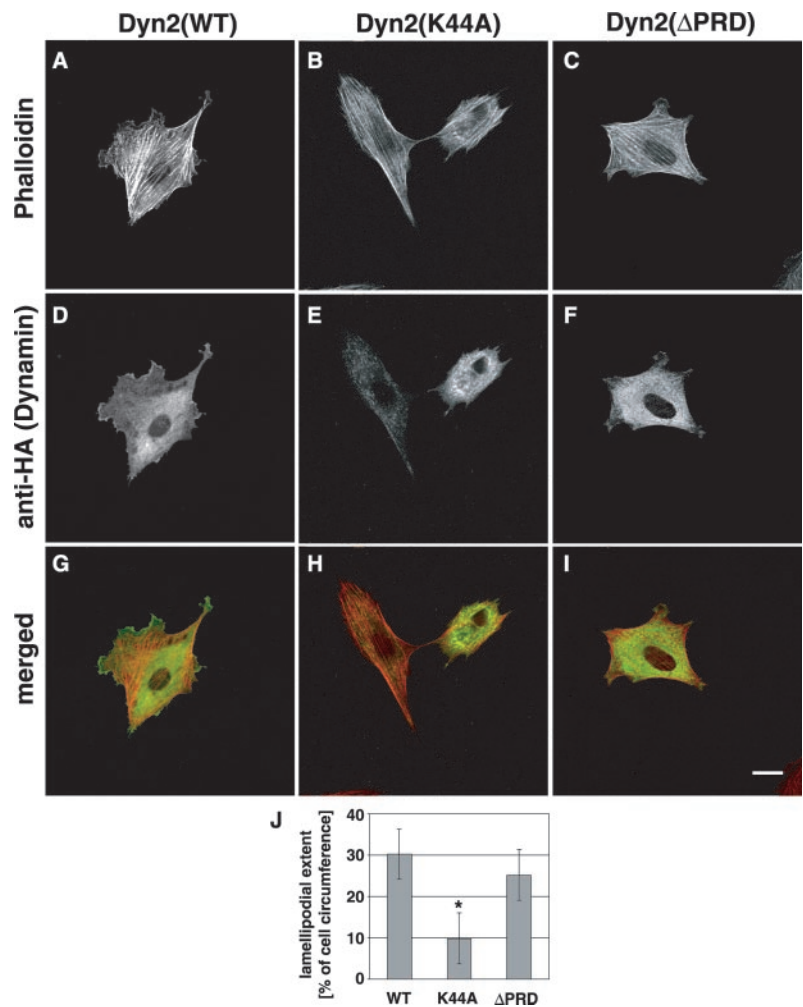


**Figure 1.** Dynamin is necessary for PDGF-induced lamellipodia. (A–I) Rat1 fibroblasts overexpressing dynamin<sup>-2</sup> constructs were plated on FN-coated coverslips, serum-starved for 16 h, stimulated with PDGF (20 ng/ml) for 30 min and stained for overexpressed dynamins (anti-HA) and filamentous actin (rhodamine-phalloidin). (J) Lamellipodial extent was quantified as fraction of cell circumference on 20 randomly selected cells in each group. Bar, 10  $\mu$ m; mean  $\pm$  SEM; \* $p$  < 0.001.

regulating protrusive actin polymerization have been envisioned (Orth and McNiven, 2003).

Lamellipodia are essential for cell spreading and migration (Bray and White, 1988). They are sites of protrusive actin polymerization and early adhesion formation initiated at the leading edge of migrating cells. The Rho-family GTPase Rac controls the formation of lamellipodia and membrane ruffles (Ridley *et al.*, 1992). Rac is also important in regulating cell growth, transcription, and apoptosis. In the cytosol, activated Rac is shielded from substrate interactions by Rho guanine nucleotide dissociation inhibitor. On integrin engagement, a specific high-affinity Rac binding site becomes available at the plasma membrane. Rac binding to this site uncouples it from Rho guanine nucleotide dissociation inhibitor, allowing for downstream signaling (Del Pozo *et al.*, 2002), which mediates actin polymerization and thus cell protrusion. Cell spreading and migration require continuous recycling of plasma membrane, Rac, and other essential signaling and structural proteins (Small *et al.*, 2002). However, little is known about the termination of Rac signaling and its relationship to membrane recycling.

In this article, we report that inhibition of dynamin-2 strongly affects Rac localization and thus, function. Dominant-negative dynamin-2 leads to the segregation of activated Rac in aberrant dorsal membrane ruffles away from cell edges to inhibit cell spreading and lamellipodia formation. Membrane-bound Rac is internalized with macropino-

somes, and platelet-derived growth factor (PDGF)-induced, Rac-dependent macropinocytosis is blocked by dominant-negative dynamin-2. These results suggest that dynamin-2 is an essential modulator of Rac localization and therefore Rac-dependent cytoskeletal remodeling.

## MATERIALS AND METHODS

### Cells and Reagents

Rat1 cells stably expressing the tetracycline-regulatable chimeric transcription activator (tTA-Rat1) were cultured in DMEM, supplemented with 5% fetal bovine serum (FBS), G418 (0.4 mg/ml) penicillin, and streptomycin. (Geneticin; Invitrogen, Carlsbad, CA). NIH3T3 cells were cultured in DMEM with 10% bovine calf serum. Recombinant adenoviruses encoding HA-dyn1WT (human dynamin-1ba splice variant), HA-dyn1K44A, HA-dyn1ΔPRD, HA-dyn2WT (rat dynamin-2ba splice variant), HA-dyn2K44A, HA-dyn2ΔPRD, HA-dyn2S45NΔPRD, HA-dyn2/1 WT-GTPase, and HA-dyn2/1 S45N-GTPase under control of a tetracycline regulatable promoter were used as described previously (Altschuler *et al.*, 1998; Fish *et al.*, 2000). For infection, tTA-Rat1 cells were incubated for 90 min with viruses at  $\sim$ 10 multiplicity of infection (m.o.i.) in serum-free DMEM. SNB19 glioblastoma cells were maintained in DMEM supplemented with 10% FBS.

### Microinjection and Transfection

NIH3T3 cells were plated on coverslips coated with fibronectin (10  $\mu$ g/ml phosphate-buffered saline [PBS]) and cells were microinjected with cDNAs encoding HA-dynamin-2(WT), HA-dynamin-2(K44A), GFP-Rac(WT), or GFP-V12Rac into their nuclei. When Rac and dynamin constructs were coexpressed, each construct was used at low doses of 0.01  $\mu$ g cDNA/ml and the cells incubated for 12–18 h. To express single Rac constructs in macropino-

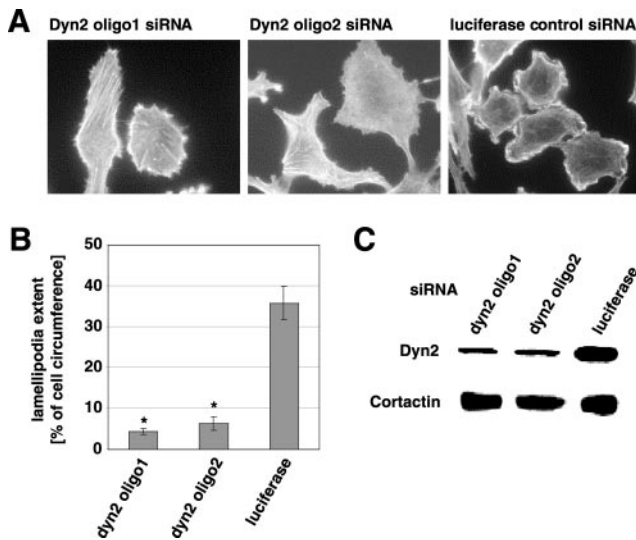


**Figure 2.** Dynamin-2 siRNA inhibits lamellipodia formation. (A) SNB 19 glioblastoma cells were plated on glass coverslips and treated with two different siRNA oligomers against dynamin 2 (dyn2) or luciferase (control) for 48 h. After serum starvation for 16 h, 52 h after transfection, cells were stimulated for 10 min with 10% FBS. After fixation in 4% formaldehyde, cells were stained with FITC-labeled phalloidin to visualize lamellipodia formation. Bar, 20  $\mu$ m. (B) Quantitation of lamellipodial extent as in Figure 1J. mean  $\pm$  SEM; \*  $p < 0.001$ . (C) SNB 19 cells were transfected with siRNA directed against either dynamin-2 or luciferase and harvested 48 h posttransfection. Expression of dynamin-2 was determined using Western blot with an anti-dynamin-2 antibody. An antibody against cortactin controls for nonspecific alterations in expression of cytoskeletal proteins.

cytosis assays (see below), 0.5  $\mu$ g cDNA/ml were injected and the cells were incubated for 90 min.

For transfection,  $2 \times 10^5$  NIH3T3 cells were seeded in 60-mm cell culture dishes and transfected with a total of 2  $\mu$ g of DNA/dish by using Effectene (QIAGEN, Valencia, CA) as recommended by the manufacturer.

### Short Interfering RNA (siRNA)

siRNAs were obtained from Dharmacon Research (Lafayette, CO). Control siRNA sequences targeted GL2 luciferase, corresponding to coding region 153–173, dynamin 2 siRNA sequences were directed against dynamin-2 at coding regions 1732–1753 for oligo 1 and at 130–151 for oligo 2. SNB19 cells were transfected with siRNAs by using oligofectAMINE (Invitrogen) as described by the manufacturer. Cells were transfected with 60 pmol of siRNA duplex per well in 24-well plates. siRNA efficiency was tested by Western blot. Cells plated at  $10^5$  cells/well were transfected with the respective siRNAs and lysed directly in Laemmli sample buffer (Bio-Rad, Hercules, CA). After separation by SDS-PAGE and transfer onto polyvinylidene difluoride membrane, membranes were incubated with either anti-dynamin-2 antibody (Santa Cruz Biotechnology, Santa Cruz, CA) at a 1:500 dilution or antibody against cortactin (Upstate Biotechnology, Lake Placid, NY) at a 1:500 dilution to control for equal amounts of protein in the samples. Standard immunoblotting was carried out using enhanced chemoluminescence (Amersham Biosciences, Piscataway, NJ).

### Lamellipodia Formation and Cell Spreading Assays

To assess lamellipodia formation, tTA-Rat1 cells overexpressing adenovirally encoded dynamin constructs were starved in 0.4% serum for 16 h and stimulated with PDGF-BB (Invitrogen) at 10 ng/ml DMEM. To test the influence of dyn2 siRNA on lamellipodia formation, SNB19 cells were plated and transfected with siRNA as described above. Twenty-four hours posttransfection, cells were trypsinized, put onto glass coverslips and allowed to adhere for another 12 h in DMEM + 10% FBS. After serum starvation for 16 h, cells were stimulated for 10 min with 10% FBS and fixed in 4% formaldehyde. To visualize the actin cytoskeleton, cells were stained with rhodamine-labeled phalloidin in PBS + 0.1% Triton X-100, and mounted using 70% Vectashield (Vector Laboratories, Burlingame, CA). To quantify lamellipodia, phalloidin-stained cells were analyzed using ISEE software (Inovision, Raleigh, NC). The

total cell periphery and the cell periphery occupied by lamellipodia as apparent in the rhodamine-phalloidin stain were outlined and measured in length. Lamellipodial extent was then expressed as percentage of total cell periphery length. Lamellipodia were identified as a smooth convex stretch of perpendicular actin stain at the peripheral edge of the cell.

For cell spreading experiments, tTA-Rat1 cells were starved in 0.4% serum for 16 h and then trypsinized and the trypsin stopped using soybean trypsin inhibitor. Cells were sedimented and resuspended in DMEM with 0.2% bovine serum albumin (BSA) and 0.4% serum and then replated onto coverslips coated with fibronectin at the indicated concentrations. To assess spreading, slide labels were blinded and all cells expressing dynamin were counted in randomly chosen fields until at least 100 cells were counted. The cells being counted were scored as “spread” or “nonspread” depending on the cell area. Nonspread cells were easily distinguished from cells that underwent spreading as nonspread cells were very small, more intensely stained and showed no lamellipodia (see also Figure 3B).

### Microscopy

NIH3T3 and Rat1 cells were plated on fibronectin-coated coverslips as indicated in the text, fixed with 2% formaldehyde for 15 min, and permeabilized with 0.2% Triton X-100/phosphate-buffered saline. Cells were stained with the respective antibodies or rhodamine-phalloidin (Molecular Probes, Eugene, OR) (0.1  $\mu$ g/ml) as indicated. Mouse monoclonal anti-hemagglutinin (HA) (Babco, Richmond, CA), anti-dynamin (HUDY-1; Warnock *et al.*, 1995) and rabbit polyclonal anti-cortactin (Santa Cruz) were used, followed by FITC- or tetramethylrhodamine B isothiocyanate-labeled secondary antibodies (Jackson ImmunoResearch Laboratories, West Grove, PA). After mounting in Immunomount C (ICN Biomedicals, Costa Mesa, CA), coverslips were viewed by fluorescence microscopy with an MC1024 (Bio-Rad, Hercules, CA) confocal laser microscope. For phase contrast and fluorescence videomicroscopy, an IX70 microscope (Olympus, Tokyo, Japan) with a CoolSNAP-Pro camera (Media Cybernetics, Silver Spring, MD) and ISEE software on a LINUX-PC were used. Live cell confocal time-lapse sequences were taken on a spinning disk confocal microscope system equipped with a 50-mW Krypton-Argon ion laser (OmniChrome; Melles Griot, Carlsbad, CA) that delivered its radiation by a single fiber optic (Point Source, Southampton, UK) to a Yokogawa spinning disk confocal scan-head (UltraView; PerkinElmer Life Sciences, Boston, MA). The system used a TE300 inverted microscope (Nikon, Tokyo, Japan) with a  $100 \times 1.4$  numerical aperture Plan-Apo differential interference objective lens (Nikon) and an Orca 2 camera (Hamamatsu, Bridgewater, NJ). MetaMorph software (Universal Imaging, Downingtown, PA) controlled the microscope functions and was used for image processing (Salmon *et al.*, 2002).

### Fluorescence Resonance Energy Transfer (FRET) Assays

Fluorescence-based in situ Rac assays were carried out as described previously (Del Pozo *et al.*, 2002). NIH3T3 cells on coverslips were microinjected with GFP-Rac together with wild-type (WT) and DN dynamin constructs as indicated. After 16–24 h to allow protein expression, 50  $\mu$ g/ml Alexa-PBD was injected into the cytosol. At 30 min, the coverslips were fixed for 15 min in 2% formaldehyde and mounted with fluoromount C (ICN Biomedicals). Images were taken with a Bio-Rad 1024 confocal microscope by using the following filters: 1) GFP-Rac, excitation 488, emission 522; 2) Alexa 546, excitation 568, emission 598; and 3) FRET excitation 488, emission 598 nm. Bleedthrough and FRET background levels were determined and subtracted as described previously (Kraynov *et al.*, 2000). Image analysis was performed using ISEE (Inovision) software on a UNIX workstation. Fluorescence intensity was displayed using a color spectrum as indicated in the scale bar.

### Rac-GTP Pull-Down Assays

tTA-Rat1 cells infected with recombinant adenoviruses as described above were incubated in DMEM with 0.4% serum for 18 h and then were chilled on ice, washed once with PBS and lysed in a buffer containing 0.5% NP-40, 50 mM Tris, pH 7.0, 150 mM NaCl, 1 mM phenylmethylsulfonyl fluoride, 1  $\mu$ g/ml aprotinin, 1  $\mu$ g/ml leupeptin, and 20  $\mu$ g of recombinant glutathione S-transferase-p21-binding domain of PAK1 (GST-PBD) as described previously (Benard *et al.*, 1999; del Pozo *et al.*, 2000). Cleared lysates were incubated with glutathione-agarose beads (Amersham Biosciences) for 30 min at 4°C, washed three times with lysis buffer, and eluted with SDS sample buffer at 95°C for 5 min. Bound Rac was analyzed by SDS-PAGE separation on a 12% polyacrylamide gel, transferred onto a nitrocellulose filter, and probed with monoclonal anti-Rac antibody (Upstate Biotechnology). For normalization, whole cell lysates were run in parallel.

### Rhodamine-Dextran Uptake

NIH3T3 cells were microinjected as described above. The cells were incubated with 0.5 mg/ml rhodamine-labeled lysine-fixable 70k-Da dextran (Molecular Probes) in regular growth medium for 30 min at 37°C, and then fixed and mounted as described above.

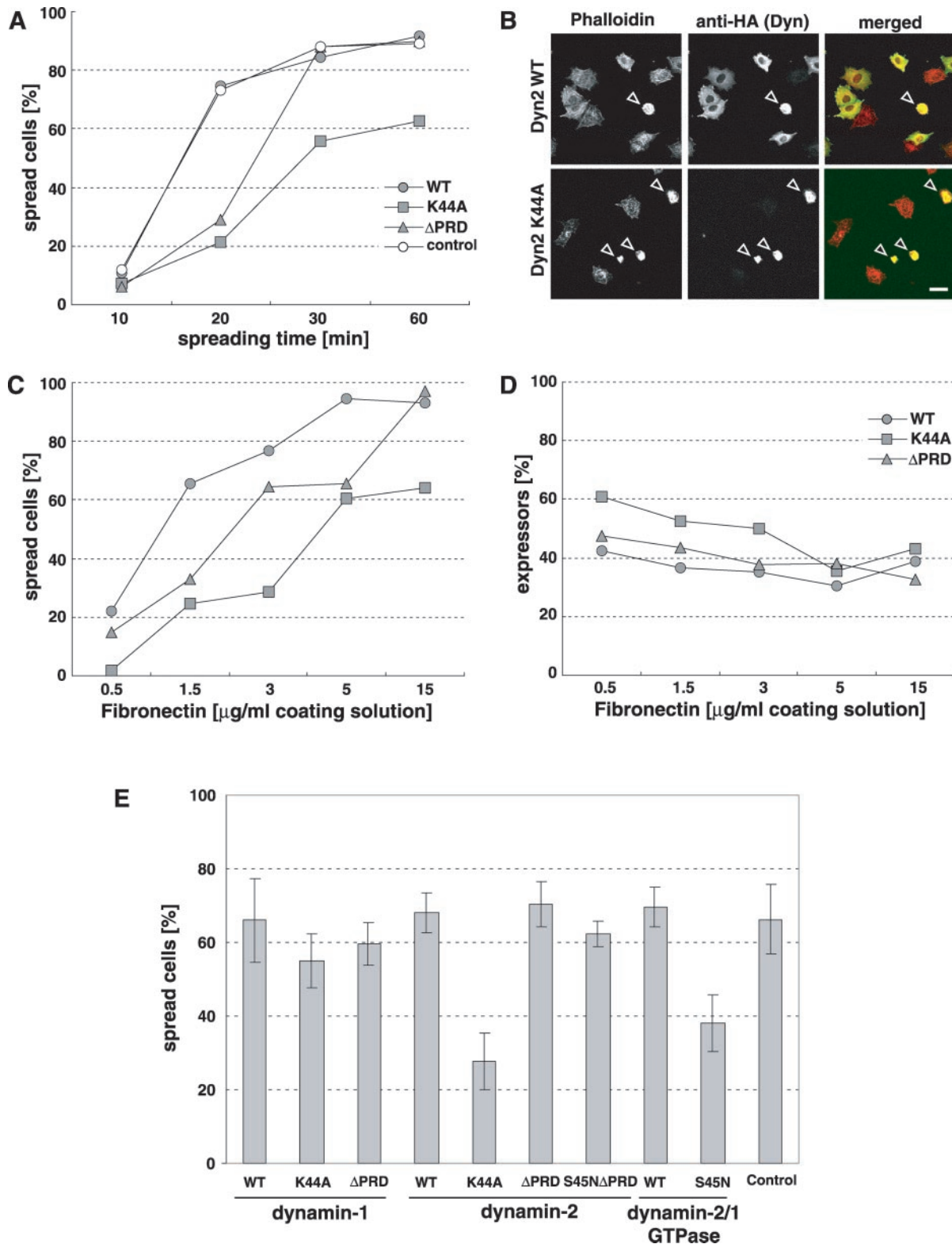


**Figure 3.** Dynamin mutants influence cell spreading but not cell adhesion. Rat1 fibroblasts overexpressing dynamin-2 constructs were serum starved for 16 h, replated on FN as indicated and stained for overexpressed dynamin and F-actin. (A) Cell spreading time course on FN-coated coverslips (15  $\mu\text{g/ml}$  coating solution). Noninfected Rat1 cells were used as control ( $n > 100$  cells for each data point). (B) Cells spreading for 20 min as in A, stained with rhodamine-phalloidin and anti-HA for overexpressed dynamin proteins. Bars, 20  $\mu\text{m}$ . (C) FN dose-response in cell spreading. (D) Effect of dynamin mutants on cell adhesion. Adherent cells were counted ( $n > 100$  for each data point) and the fraction of cells overexpressing dynamin constructs was determined. Results are representative of three experiments (A–D). (E) Comparison of dynamin constructs in cell spreading on FN (15  $\mu\text{g/ml}$  coating solution) for 30 min. Noninfected Rat1 cells served as control. Results are means  $\pm$  SEM from three experiments.

### Quantification of Pinocytosis by Horseradish Peroxidase (HRP) Uptake Assays

For the analysis of fluid phase uptake, tTA-Rat1 cells were grown on 35-mm plates. Cells were starved in 0.4% serum for 16 h. During this time cells were infected with the appropriate adenoviruses (~10 m.o.i.) in the absence or presence of tetracycline (1  $\mu$ g/ml). Cells were incubated with 4 mg/ml HRP in DMEM with 20 mM HEPES, 0.2% BSA, pH 7.4, for 7 min at 37°C or 4°C  $\pm$  PDGF-BB at 20 ng/ml (Invitrogen). The uptake was stopped by quick aspiration of the medium and five washes with PBS, 1 mM MgCl<sub>2</sub>, 1 mM CaCl<sub>2</sub>, 0.2% BSA, pH 7.4, for 5 min at 4°C and 2 short rinses with PBS at 4°C. The cells were then treated with 0.1% pronase in PBS, pH 7.4, to detach cells and remove residual HRP nonspecifically bound to the plasma membrane. Cell suspensions were then spun at 4°C through a sucrose cushion (0.5 M in PBS, pH 7.4) for 5 min at 1,000 rpm followed by 20 s at 14,000 rpm. The cells were lysed in PBS, 0.5% Triton X-100, and aliquots were assayed for enzyme activity (A490 nm) by using *o*-phenylenediamine as a substrate and for protein concentration (A600 nm) using the MicroBCA assay (Pierce Chemical, Rockford, IL).

## RESULTS

### Dynamin Function Is Necessary for Lamellipodia Formation

Dynamin has been shown to localize to the leading edge of growth factor-stimulated migrating cells (Cao *et al.*, 1998; McNiven *et al.*, 2000a). To investigate the functional significance of dynamin localization to lamellipodia, we assessed the influence of dynamin mutants. Rat1 cells constitutively expressing a tetracycline transactivator (tTA) were infected with recombinant adenoviruses encoding dyn2(WT), dominant-negative dyn2(K44A) or dyn2( $\Delta$ PRD) lacking the C-terminal proline-, arginine-rich domain. The proline-arginine-rich domain (PRD) mediates binding to cortactin and other SH3 domain-containing proteins that are critical to dynamin function (McNiven *et al.*, 2000b). The adenoviral expression system allows for highly reproducible protein overexpression. Proteins were expressed for 18 h in cells plated on fibronectin in 0.4% FBS. To induce lamellipodia, 20 ng/ml PDGF was applied for 30 min. Cells expressing dyn2(WT) formed large lamellipodia that comprised an average of 30% of the cell circumference (Figure 1, A, D, G, and J). At these times after infection, dyn2(WT) cells were not noticeably different from untransfected cells (our unpublished data). In contrast, expression of dyn2(K44A) significantly inhibited the formation of lamellipodia in response to PDGF (9.8% of cell circumference,  $p < 0.001$ ; Figure 1, B, E, H, and J). Dyn2( $\Delta$ PRD)-expressing cells formed slightly smaller lamellipodia (25% of cell circumference), but the effect was statistically insignificant (Figure 1, C, F, I, and J). The expression levels for dynamin constructs were equal under these conditions as determined by Western blot (our unpublished data; but see Figure 4).

As an alternative approach, we used siRNA-mediated gene silencing to decrease dynamin-2 levels in cells. Human SNB19 glioblastoma cells were chosen for their high siRNA transfection efficiency. Cells treated with two different dynamin-2 siRNA oligomers decreased dyn2 expression by 80% without altering the expression levels of the dynamin-interacting cytoskeletal protein cortactin (Figure 2C), clathrin adapter protein-2 or dynamin 1 (our unpublished data). Treated cells failed to form lamellipodia upon serum stimulation (Figure 2A). The effect of both dyn2 siRNA oligomers on lamellipodia formation was significant compared with control siRNA (Figure 2B). We also observed that siRNA-mediated down-regulation of dynamin-2 inhibited cell spreading in several cell types (our unpublished data). Thus, blocking of dynamin-2 function either by overexpression of a dominant-negative mutant or by suppression of endogenous dynamin-2 expression inhibits lamellipodia formation.

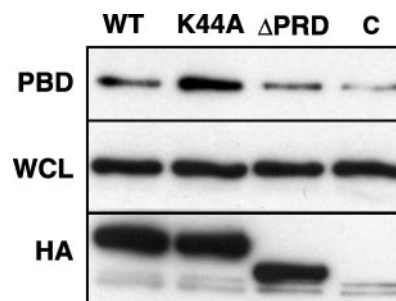


**Figure 4.** Dominant-negative dyn2(K44A) leads to increased Rac activity. Rat1 cells overexpressing dynamin constructs were starved in 0.4% serum for 16 h, lysed, and active Rac was assessed in a GST-PBD pull-down assay. Noninfected cells served as control. Active Rac (PBD), total Rac (WCL), and dynamin construct expression levels (HA) were detected by Western blot. Results are representative of three experiments.

### Dynamin Mutants Influence Cell Spreading but Not Cell Adhesion

Lamellipodia mediate cell spreading (Price *et al.*, 1998); thus, we tested the influence of dynamin mutants on integrin-mediated cell adhesion and spreading. In these experiments, we used a low m.o.i. so that only 40–50% of the cells expressed dynamin constructs at levels detectable by anti-HA immunofluorescence microscopy, thereby providing an additional control. When plated on a surface coated with 15  $\mu$ g fibronectin/ml, noninfected control cells and cells overexpressing dyn2(WT) spread equally well (Figure 3A). Overexpression of dyn2( $\Delta$ PRD) delayed spreading but cells spread fully at later times. Only those cells that showed appreciable dyn2( $\Delta$ PRD) staining were delayed in spreading; low or nonexpressors in the same population were unaffected. In contrast, overexpression of dyn2(K44A) inhibited cell spreading at all times examined. Figure 3B shows typical fields with cells expressing either dyn2(WT) or dyn2(K44A) 20 min after replating on fibronectin (FN).

Changes in integrin activation state or surface expression could conceivably account for these results. Either of these alterations should result in decreased adhesion and a shift in the dose response to FN. We therefore measured cell adhesion and spreading on various concentrations of FN. Serum-starved cells were plated for 60 min and then fixed and stained for dynamin expression by using an anti-HA antibody and for F-actin by using rhodamine-phalloidin. In random microscopic fields, all dynamin expressors were counted and scored as spread or nonspread (Figure 3, A and C). The fraction of adherent cells expressing dynamin was taken as an indication of cell adhesion (Figure 3D). As before, dyn2(K44A) overexpression strongly inhibited cell spreading compared with dyn2(WT) (Figure 3C). Dyn2( $\Delta$ PRD) overexpression gave a smaller degree of inhibition. However, no shift in the dose-response curves for FN was detected. Importantly, no decrease in the proportion of expressing cells was observed even at low concentrations of FN (Figure 3D). The slight apparent increase in percentage of transfected cells at low FN density probably reflects increased brightness of round cells that makes low expressors more apparent. This is most obvious with dyn2(K44A), where greater numbers of poorly spread cells were present. We conclude that dyn2(K44A) and dyn2( $\Delta$ PRD) did not significantly affect integrin function.

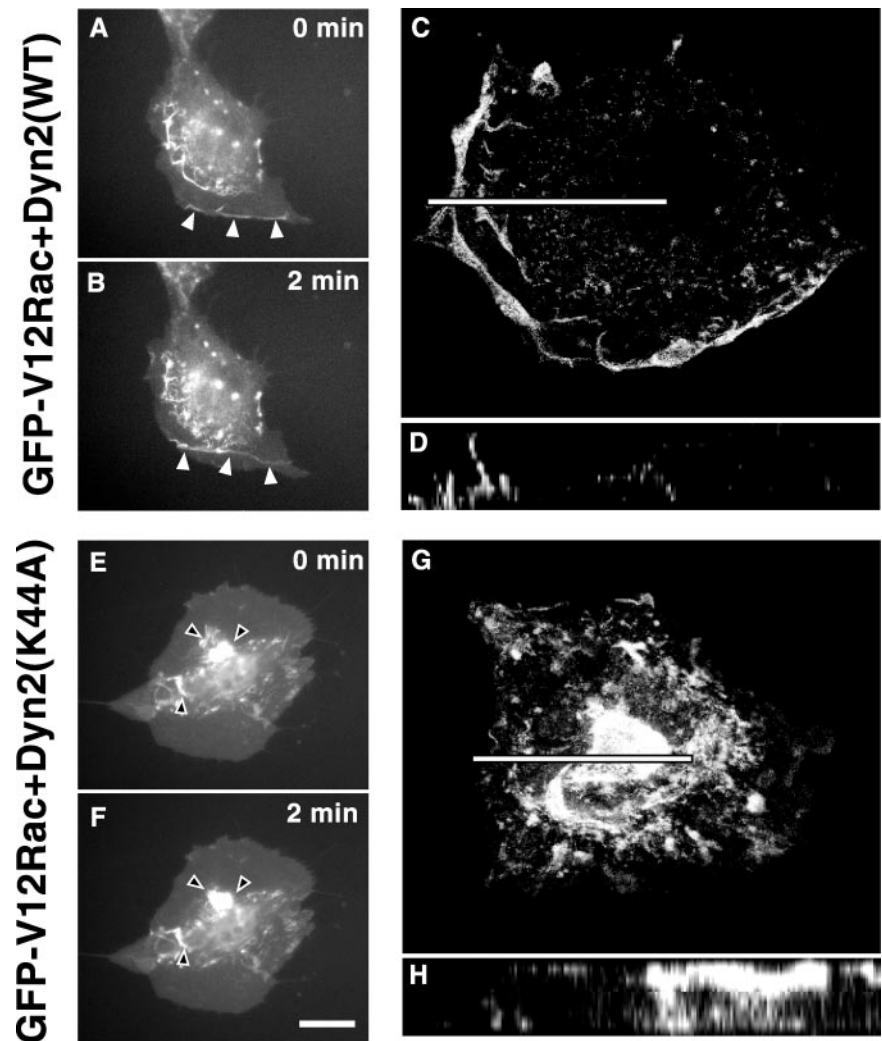


**Figure 5.** Dominant-negative dyn2(K44A) induces Rac mislocalization. NIH3T3 fibroblasts were injected with plasmids encoding GFP-tagged constitutively active V12Rac and either dyn2(WT) or dyn2(K44A). When the GFP signal indicated proper protein expression, phase contrast and GFP-V12Rac fluorescence images were taken once per minute with a videomicroscope. Arrowheads indicate typical peripheral membrane ruffles (A and B) and abnormal dorsal ruffles (E and F), respectively. Images (A, B, E, and F) are frames of time-lapse videos available as supplemental material. Bar, 20  $\mu\text{m}$ . To characterize the localization of the Rac signal in the ruffles, cells were fixed, stained, evaluated with confocal microscopy (C, D, G, and H), and z-axis reconstructions (D and H) were generated along the bars indicated in C and G. Bar (C), 30  $\mu\text{m}$ ; (G), 25  $\mu\text{m}$ .

#### *Isoform Specificity and the Role of the Proline-Arginine-rich Domain*

We also examined effects of dynamin-1 in spreading assays (Figure 3E). Dominant-negative constructs of dynamin-1 and -2 isoforms are equally effective at blocking clathrin-dependent and clathrin-independent endocytosis (Altschuler *et al.*, 1998; Lamaze *et al.*, 2001; Pelkmans *et al.*, 2002). Surprisingly, dyn1(K44A) was much less effective than dyn2(K44A) at inhibiting cell spreading. Given that the inhibitory effects of dynamin-2 were due to mutations in its GTPase domain, we investigated the basis for this functional difference by generating GTPase domain chimeras of dynamin-1 and -2. Thus, we replaced the dynamin-1 GTPase domain with the GTPase domain of dynamin-2, with or without the S45N dominant-negative mutation (dyn2/1). The K44A and S45N mutations both inactivate the GTPase domain and can be used equivalently in cell spreading experiments (our unpublished data). Control experiments showed that the dyn2/1(S45N) mutant chimera inhibited clathrin-mediated endocytosis as potently as dyn2(S45N) (our unpublished data). Similarly, cell spreading was also strongly inhibited in cells expressing the dyn2/dyn1(S45N) chimera, but not the dyn2/dyn1(WT) chimera. Thus, the difference between dynamin-1 and -2 correlates with the GTPase domain. Interestingly, this difference occurs even

though the GTPase domains of dynamin-1 and dynamin-2 are 88% identical. These data also indicate that the 399–444 splice site is not critical to these effects, because we used dyn1(aa) and dyn2(ba) splice variants and a chimeric dyn2/dyn1(S45N)(aa) construct.

Dynamin-1 and -2 interact with numerous SH3 domain-containing partner molecules through their C-terminal PRD. To determine whether these interactions were necessary for the inhibitory effects of DN-dynamin-2, we generated a double mutant lacking the C-terminal PRD and bearing the inactivating S45N mutation in the GTPase domain. This double mutant potently inhibited clathrin-mediated endocytosis (unpublished data), but failed to inhibit cell spreading (Figure 3E). Thus, interactions via the PRD, which are lost in the double mutant, are also necessary to exert a dominant-negative effect on cell spreading. These results further distinguish effects on cell spreading from those on clathrin-mediated endocytosis.

#### *Dominant-negative Dyn2(K44A) Leads to Increased Total Rac Activation*

Rac activity is essential for cell spreading and lamellipodia formation (Ridley *et al.*, 1992; Price *et al.*, 1998). Given that integrin function seemed unaffected, we next investigated the effects of dynamin mutants on total Rac activation (Fig-

ure 4). Dyn2(WT), dyn2(K44A), and dyn2( $\Delta$ PRD) were expressed in tTA-Rat1 cells as described above. Similar expression levels were obtained for all constructs. After overnight starvation in 0.4% serum, cell lysates were prepared, active Rac was precipitated with GST-PBD and analyzed by Western blot. To our surprise, overexpression of dyn2(K44A) led to increased Rac activation compared with dyn2(WT) and dyn2( $\Delta$ PRD) (Figure 4), despite the inhibition of Rac-dependent lamellipodia formation (Figure 1).

#### *Dyn2(K44A) Induces Mislocalization of Rac*

Despite increased total Rac activation, Rac signaling seemed to be perturbed by dominant-negative dynamin. One possible explanation is that the activated Rac is mislocalized. To visualize Rac localization and to test whether constitutively active Rac could override a possible effect of dominant-negative dynamin, NIH3T3 cells were microinjected with plasmids coding for constitutively active GFP-V12Rac together with dyn2(WT) or dyn2(K44A) (Figure 5). Microinjection of cDNA in NIH3T3 cells allowed for reliable coexpression of different constructs. When coexpressed with dyn2(WT), GFP-V12Rac induced typical lamellipodia and dorsal membrane ruffles that originated at the cell edge and moved rapidly toward the center of the cell where they dissipated (arrowheads in Figure 5, A and B, and Video 1; another example with z-axis reconstruction in Figure 5, C and D). In contrast, coexpression of dyn2(K44A) and GFP-V12Rac abolished membrane ruffling at the cell edges. Instead, abnormal, irregularly shaped, ruffles enriched in GFP-V12Rac were prevalent in the central region of the dorsal surface and could be seen moving slowly in time lapse imaging (arrowheads in Figure 5, E and F, and Video 2). The movement is not centripetal as for regular ruffles and their localization to the central part of the apical surface is unusual (Figure 5, G and H). GFP-Rac(WT) was similarly mislocalized with dyn2(K44A) expression (our unpublished data; but see Figure 6).

#### *Rac Mislocalized by dyn2(K44A) Is Active*

To gain further insight into the effects of dyn2(K44A), the subcellular distribution of Rac activity was visualized using a recently developed FRET assay (Figure 6). When GFP-Rac(WT) was coexpressed with dyn2(WT), the active Rac was localized at lamellipodia and membrane ruffles and in a perinuclear region as described previously (Figure 6, A, B, and E) (Kraynov *et al.*, 2000). When GFP-Rac(WT) was expressed with dyn2(K44A), Rac activity was markedly higher but absent from cell edges, instead being concentrated in zones corresponding to the abnormal membrane ruffles seen with GFP-V12Rac (Figure 6, C–E). To quantitate these observations, cells were scored for the presence or absence of FRET-positive central or peripheral ruffles (Figure 6E). The analysis shows that dyn2(K44A) causes loss of peripheral ruffles and appearance of central ruffles.

#### *Dyn2(K44A) Induces Accumulation of Membrane-bound Rac in Tubulo-vesicular Structures*

To explore the translocation of Rac from the plasma membrane and possible effects of dominant-negative dynamin-2 on Rac trafficking in more detail, we studied the spatiotemporal distribution of GFP-Rac(WT) with high-resolution confocal time-lapse microscopy. The cells were studied at early time points of dynamin expression (12–14 h after low-dose injection as opposed to 18 h), before the aberrant ruffle phenotype was apparent, to capture the origin of this phenotype.

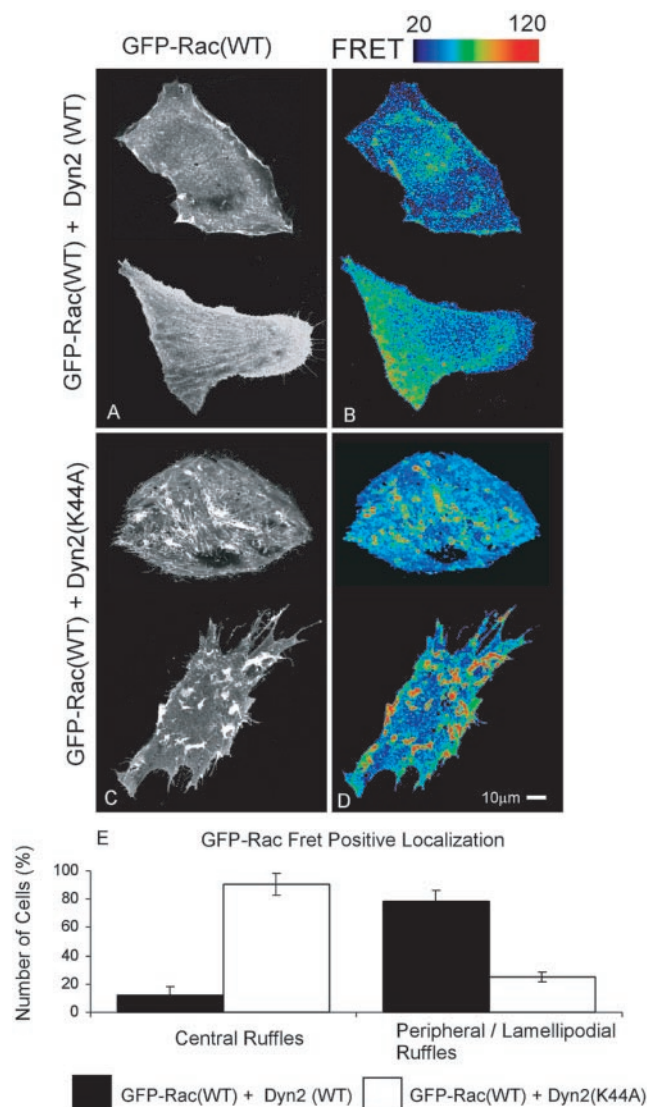
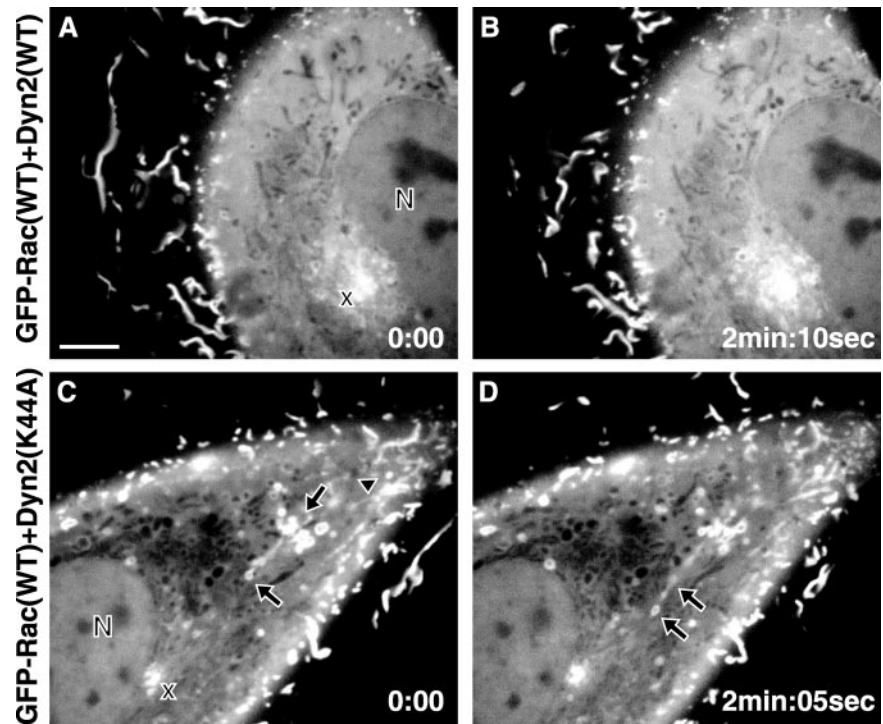


**Figure 6.** Rac mislocalized by dyn2(K44A) overexpression is active. NIH3T3 cells containing wild-type Rac-GFP, dyn2(WT) (A and B) or dyn2(K44A) (C and D) were analyzed. Corrected FRET images are representative of four independent experiments. FRET signal intensity from 20 to 120 is displayed using pseudocolor as indicated by the scale bar. Blue represents low and red high FRET signal. (E) Scoring of FRET signal localization. Cells were scored for presence or absence of central and peripheral FRET-positive ruffles. Values are means of four independent experiments  $\pm$  SEM, 50 cells/group were assessed in each experiment.

When GFP-Rac(WT) was coexpressed with dyn2(WT), a distinct GFP-Rac signal was apparent in peripheral membrane ruffles moving centripetally, the cytosol contained diffuse GFP-Rac and dark tubular organelles (Figure 7, A and B). The perinuclear zone was enriched in GFP-Rac and tiny puncta of GFP-Rac seemed to move centripetally toward this zone. Very few larger vesicles bearing membrane-bound GFP-Rac were present. When dominant-negative dyn2(K44A), which inhibits the severing of membrane vesicles, was expressed with GFP-Rac(WT), fewer peripheral ruffles were observed, streaks of GFP-Rac signal stretched from the cell membrane into the cytoplasm (Figure 7, C and D, arrowhead), and, most strikingly, tubulo-vesicular struc-

**Figure 7.** GFP-Rac(WT) trafficking in the presence of dyn2(WT) and dyn2(K44A). NIH3T3 cells were microinjected with plasmids encoding GFP-Rac(WT) and Dyn2(WT) or Dyn2(K44A). The GFP-Rac(WT) signal was recorded in a time lapse series with a high-resolution spinning disk confocal microscope at the onset of protein expression, before abnormal ruffles became apparent with dyn2(K44A). N, nucleus; x, perinuclear GFP-Rac(WT)-enriched region; arrowhead, GFP-Rac(WT) signal streaks emanating from the zone of membrane ruffles; arrows, tubulo-vesicular structures bearing a membrane-associated GFP-Rac(WT) signal. Time-lapse videos are available as supplemental material. Bar, 5  $\mu$ m, time as minutes:seconds.



tures positive for GFP-Rac accumulated in the cytoplasm (Figure 7, C and D, arrows). At the same time, punctate GFP-Rac was diminished in the perinuclear zone (Figure 7, C and D, "x"). These data argue that mutant dynamin alters the inward vesicular transport of GFP-Rac(WT). One vesicle is depicted pinching off the tubulo-vesicular complex toward the diminished perinuclear zone (Figure 7D, left arrow).

#### **Membrane-bound Activated Rac Is Internalized with Macropinosomes**

The confocal time-lapse images suggested a vesicular internalization of membrane-bound Rac from the plasma membrane and its inhibition by dominant-negative dyn2(K44A). In a process induced downstream of Rac, ruffling membrane is internalized via the formation of macropinosomatic vesicles (Swanson and Watts, 1995; Dharmawardhane *et al.*, 2000). To study a possible link between macropinosomes and Rac trafficking, we next assessed macropinosomes for the presence of membrane-bound Rac. NIH3T3 cells were injected with plasmids coding for constitutively active GFP-V12Rac or GFP-Rac(WT). After 90 min of protein expression, the cells were incubated with rhodamine-labeled 70-kDa dextran for 30 min, fixed and evaluated by confocal microscopy. Indeed, constitutively active GFP-V12Rac was found on the membranes of macropinosomatic vesicles (Figure 8, A–D). By contrast, GFP-Rac(WT) was not strongly associated with macropinosomes (Figure 8, E–H), although some macropinosomes were associated with a much weaker punctate GFP-Rac(WT) signal.

#### **Dyn2(K44A) Inhibits Rac-dependent, PDGF-induced Macropinosomes**

Given that dynamin is generally critical for internalization of plasma membrane, the above-mentioned effects of K44A dynamin could be explained if ruffling membrane were

trapped at the cell surface and could not internalize in macropinosomes. To test this hypothesis, we assessed macropinosomes in NIH3T3 cells microinjected with plasmids encoding constitutively active GFP-V12Rac and dyn2(WT) or dyn2(K44A). After proteins were expressed, the cells were incubated with rhodamine-dextran for 30 min, fixed, and evaluated by confocal microscopy. When coexpressed with dyn2(WT), GFP-V12Rac induced membrane ruffles (Figure 9A) and increased uptake of rhodamine-dextran (Figure 9A, right, arrowheads). When high levels of dyn2(K44A) were coexpressed, GFP-V12Rac was mislocalized as shown above (Figure 9A, arrow), and rhodamine-dextran uptake was comparable to noninjected, unstimulated cells. Those cells that had only low levels of dyn2(K44A) retained normal GFP-V12Rac localization (Figure 9A, left, arrowhead) and showed increased rhodamine-dextran uptake similar to dyn2(WT)-expressing cells. This effect is therefore dose dependent.

To quantitate macropinosomatic activity in response to a physiological stimulus, PDGF-stimulated fluid phase uptake of HRP was measured (Figure 9B). Incubation of cells with PDGF, which is known to activate Rac (Ridley *et al.*, 1992; Hawkins *et al.*, 1995; Sander *et al.*, 1999), increased fluid phase uptake by approximately twofold. This increase was completely abolished by dyn2(K44A) expression but only partially reduced by expression of dyn1(K44A) (Figure 9B) and was not inhibited by overexpression of the double mutant, dyn2(S45N/ $\Delta$ PRD). Basal rates of fluid-phase endocytosis are largely unaffected by overexpression of either of these mutants (Figure 9B), even though all of them effectively inhibit clathrin-mediated endocytosis (our unpublished data). Importantly, the isoform specificity and structural requirements for inhibition of Rac-induced macropinosomes paralleled those found for inhibition of integrin-dependent lamellipodia formation and cell spreading (Figure 3E).



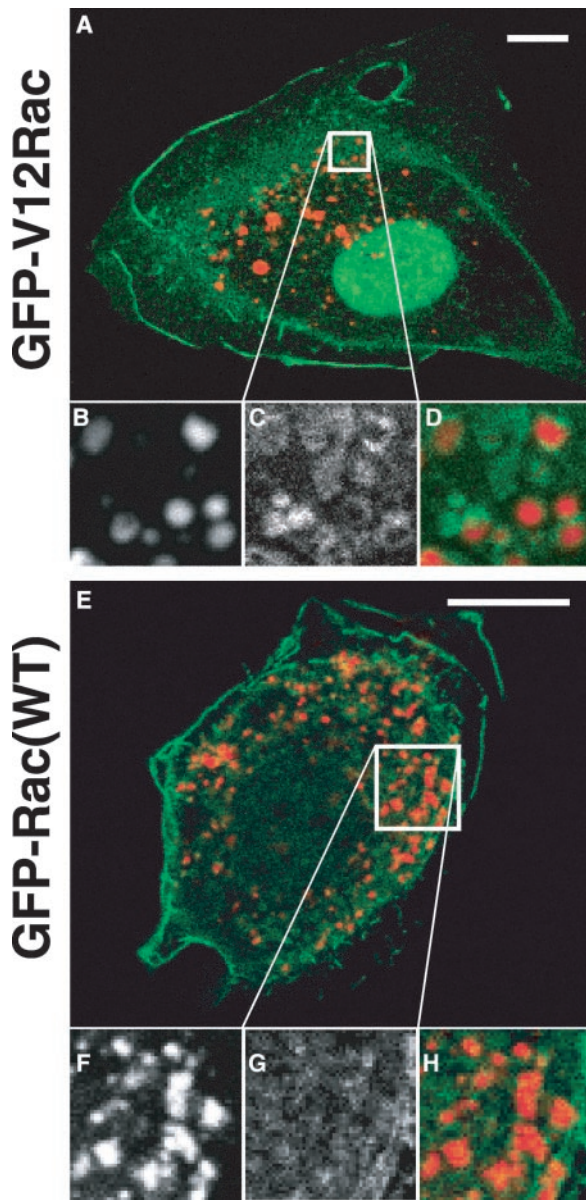


**Figure 8.** Membrane-bound Rac is internalized with macropinosomes. NIH3T3 cells were microinjected with plasmids encoding GFP-V12Rac or GFP-Rac(WT), incubated for 90 min, exposed to rhodamine-labeled 70-kDa dextran (0.5 mg/ml) for 30 min, fixed, mounted, and subjected to confocal microscopy. (B–D) Close-up as indicated in A. (F–H) Close-up as indicated in E. (B and F) Rhodamine-dextran indicating pinosomes. (C) GFP-V12Rac. (G) GFP-Rac(WT). (A, D, E, and H) Merged images. Bars, 10  $\mu$ m.

## DISCUSSION

The large GTPase dynamin and the Rho-family GTPase Rac are both involved in cytoskeletal regulation (Ridley *et al.*, 1992; Orth and McNiven, 2003). We now provide evidence that dynamin is able to modulate Rac function. Dynamin localizes to lamellipodia and membrane ruffles (Cao *et al.*, 1998; McNiven *et al.*, 2000b) in spatio-temporal synchrony with Rac. Integrin engagement actuates Rac downstream signaling (Price *et al.*, 1998; Del Pozo *et al.*, 2002) to drive lamellipodia formation. Integrin stimulation is sufficient to

recruit dynamin to lamellipodia, even in the absence of growth factors (our unpublished data).

Our data indicate that dynamin-2 is essential for lamellipodia formation and cell spreading. When dynamin function was disrupted by expression of a dominant-negative mutant, integrin-mediated (Figure 3) as well as growth factor-dependent induction of lamellipodia were abolished (Figure 1). Similarly, an siRNA-induced reduction in dynamin-2 inhibited growth-factor induced lamellipodia formation (Figure 2). Alterations in integrin activity or signaling (Price *et al.*, 1998) could conceivably account for these findings, however, neither the rate of cells adhering to fibronectin, nor the dose response to fibronectin was significantly altered by dominant-negative dynamin. Thus, integrin function per se seems unaffected.

Because some dynamin-mediated effects are isoform specific (Cao *et al.*, 1998; Fish *et al.*, 2000), we compared dynamin-1 and -2 isoforms in cell spreading experiments (Figure 3E). Dominant-negative dyn2(K44A) inhibited cell spreading to a much greater extent than dyn1(K44A). Dynamin-1 and dynamin-2 are ~70% identical, with the greatest sequence divergence occurring in the C-terminal proline-, arginine-rich domain and within splice variants located in the middle domain. Thus, it was surprising that a chimeric molecule consisting of dynamin-1 with the dyn2(S45N) GTPase domain was almost as potent as full-length dyn2(S45N). Based on these data, we speculate that effectors of the GTPase domain might be required for the specific dominant-negative effects of dynamin-2 on cell spreading. In addition to specific interactions of the dynamin-2 GTPase domain, inhibition of cell spreading required the C-terminal PRD. These data therefore suggest that both the GTPase and the SH3-binding PRD contribute to lamellipodia formation. Although the dominant-negative mutants dyn2(S45N $\Delta$ PRD) and dyn1(K44A) both strongly inhibit clathrin-mediated endocytosis, they had no significant effect on cell spreading and Rac-induced macropinosytosis. We conclude that the modulation of Rac localization by dynamin differs from clathrin-mediated endocytosis and that dynamin functions in a distinct manner in these different membrane-trafficking events.

Loss of lamellipodia could indicate a blockade of Rac activation. However, dominant-negative dynamin led to increased total Rac activity (Figure 4). Because Rac localization is also critical for downstream signaling (del Pozo *et al.*, 2000), we examined the subcellular distribution of green fluorescent protein (GFP)-tagged Rac in the presence of dynamin mutants (Figure 5). Dominant-negative dynamin induced Rac mislocalization to aberrant dorsal membrane ruffles. The expression of constitutively active GFP-V12Rac could not override the effect of dyn2(K44A). These data and results from FRET assays (Figure 6) indicate that dyn2(K44A) leads to sequestration of active Rac in aberrant membrane ruffles. At the same time, an increase in total Rac activity suggests either a failure in Rac deactivation or an abnormal activation of Rac.

Confocal time-lapse microscopy of GFP-Rac constructs at the onset of dynamin construct expression provided some insights into the effects of dominant-negative dynamin on Rac dynamics. With dyn2(WT), punctate GFP-Rac(WT) signals seem close to the plasma membrane and some move toward a perinuclear region enriched in Rac. It is not clear whether this perinuclear zone is an endosomal recycling compartment, part of the Golgi apparatus, or both. Dyn2(K44A), however, attenuates the perinuclear accumulation of Rac and leads to streaks of Rac signal emanating from the plasma membrane region and to the accumulation

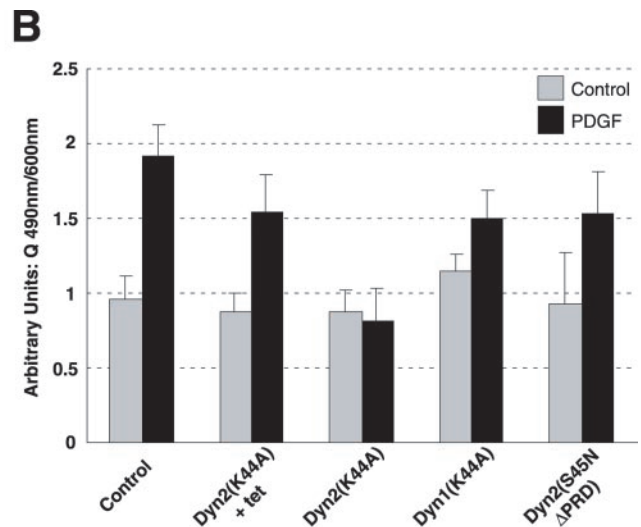
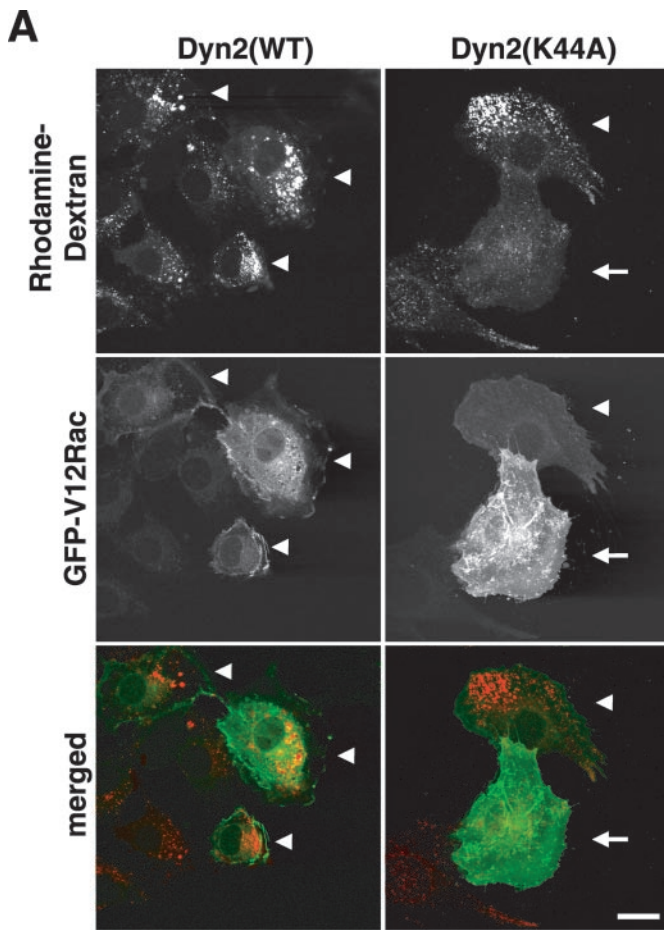


**Figure 9.** Dyn2(K44A) inhibits PDGF-induced macropinocytosis. (A) NIH3T3 cells were microinjected with plasmids encoding GFP-V12Rac and Dyn2(WT) or Dyn2(K44A). When the GFP signal indicated proper expression, the cells were incubated with rhodamine-labeled dextran for 30 min. (B) HRP uptake assay. Rat1 cells expressing dynamin constructs were serum starved, and HRP uptake was measured 10 min after stimulation with PDGF (20 ng/ml) or vehicle. Results are mean  $\pm$  SEM of three independent experiments.

of tubulo-vesicular structures that are positive for GFP-Rac(WT). The tubular structures seen with dyn2(K44A) are consistent with the well characterized effect of dominant-negative dynamin on membrane structures of nascent vesicles (Damke *et al.*, 2001). When vesicle fission is retarded but not yet fully blocked at the onset of dyn2(K44A) expression, small unsevered vesicles elongate and grow to larger vesiculotubular complexes. These data suggest that in the presence of dyn2(WT), Rac is internalized in small vesicles and that this process is perturbed by dominant-negative dynamin. The finding that dominant-negative dynamin does not affect outward transport of vesicles from the Golgi to the plasma membrane (Altschuler *et al.*, 1998), together with the depletion of perinuclear Rac-containing vesicles, argues against direct inhibition of outward transport of Rac to the plasma membrane.

Macropinosomes are vesicular structures that arise from membrane ruffles (Swanson, 1989) in a process mediated by the Rac effector PAK (Dharmawardhane *et al.*, 2000). Thus, macropinosomes are a candidate vehicle for Rac internalization from membrane ruffles that might be susceptible to modulation by dynamin. We found that GFP-V12Rac is internalized with macropinosomes (Figure 8). Because the constitutively active mutant GFP-V12Rac cannot be deactivated, it remains membrane-bound, allowing for its detection on macropinosomes. GFP-Rac(WT), by contrast, can be rapidly deactivated, leading to its dissociation from membranes so that only a very weak GFP-Rac(WT) signal could be detected in association with some macropinosomes.

Dominant-negative dyn2(K44A) specifically inhibited V12Rac- or PDGF-induced macropinocytosis without affecting baseline fluid phase uptake (Figure 9). This result is consistent with the idea that plasma membrane internalization is impaired by dominant-negative dyn2(K44A). We have shown (Damke *et al.*, 1995; Altschuler *et al.*, 1998) that a compensatory, dyn1- and dyn2-insensitive and clathrin-independent fluid phase endocytic mechanism is induced after inhibiting clathrin-mediated endocytosis by either dyn1(K44A) or dyn2(K44A). The results in this article confirm that neither dyn1(K44A) nor dyn2(K44A) inhibit this baseline constitutive fluid phase uptake mechanism but that dyn2(K44A) specifically inhibits the PDGF-induced component of fluid phase uptake. Importantly, clathrin-dependent endocytosis is strongly inhibited by the dominant-negative double mutant dyn2(S45N DPRD) and by dyn1(K44A), but these constructs had little or no effect on PDGF-induced HRP uptake. This correlates well with the isoform-specific effects on cell spreading. Thus, we conclude that disruption of dynamin function inhibits the internalization of Rac from the plasma membrane and leads to the accumulation of activated Rac in abnormal membrane ruffles, depleting Rac needed for the formation of new lamellipodia (Figure 10).

Rac was recently reported to be in dynamin immunoprecipitates after PDGF stimulation (Krueger *et al.*, 2003). However, we did not detect coimmunoprecipitation of Rac and HA-tagged overexpressed dynamin after PDGF-stimulation in our system (our unpublished data). Because the antibodies and systems used are different, an interaction of Rac and

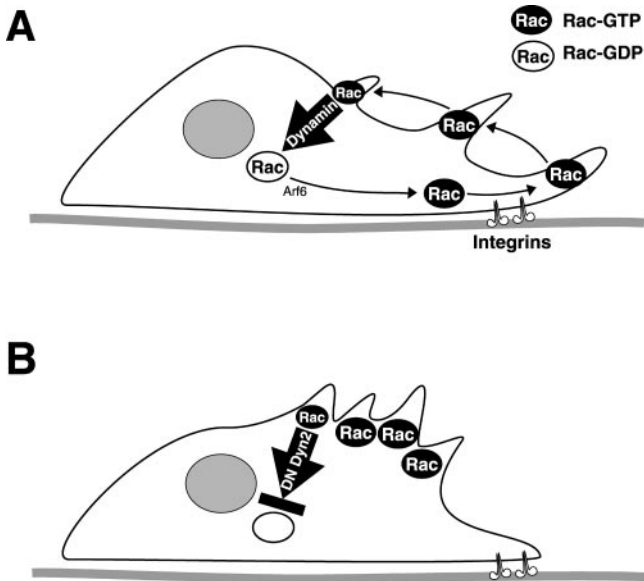


**Figure 10.** Model for dynamin-dependent Rac localization. (A) Rac has been localized to an ARF-6-dependent endosomal-plasma membrane recycling pathway (Radhakrishna *et al.*, 1999). In migrating and spreading cells, integrins control binding sites for active Rac at the plasma membrane to induce lamellipodia and membrane ruffles (Del Pozo *et al.*, 2002). Peripheral ruffles move centripetally and give rise to macropinosomes. Rac is internalized with macropinosomes in a dynamin-dependent manner as a prerequisite for its deactivation and recycling. (B) Dominant-negative dynamin<sup>-2</sup> (DN Dyn2) inhibits Rac internalization leading to segregation of activated Rac into aberrant dorsal membrane ruffles. Subsequently, the Rac recycling pathway is depleted and lamellipodia formation subsides.

dynamin in a protein complex is a possibility. Dynamin-2-dependent internalization of membrane-bound Rac could be a prerequisite to GAP-mediated Rac deactivation in a specialized protein complex or subcellular compartment. Rac signaling is terminated by GTPase-activating proteins that act in a spatio-temporally regulated manner. The accumulation of membrane-associated GFP-Rac(WT) on tubulated cytoplasmic vesicles and streaks emanating from the zone of membrane ruffling seen with early dyn2(K44A) expression (Figure 7, C and D, and Video 4) is consistent with this hypothesis. The presence of constitutively active but not WT Rac on the membrane of macropinosomes further strengthens this idea (Figure 8). Finally, an inhibition of Rac- or PDGF-dependent macropinocytosis by dyn2(K44A) (Figure 9) indicates a role for dynamin in the pinocytotic internalization of membranes from ruffles, a mechanism that can serve to translocate Rac.

Further work will be required to elucidate the mechanism by which dynamin-2 controls Rac activity and localization. However, our results connect dynamin's known function in membrane trafficking to Rac localization and function, providing a new functional link between dynamin and regulation of the actin cytoskeleton.

## ACKNOWLEDGMENTS

This work was supported by Deutsche Forschungsgemeinschaft fellowship Schl563/1-1,1-2 (to G.S.), California Cancer Research Program 00-00743V-20070 (to H.D.), American Heart Association fellowship 0120068Y (to W.B.K.), National Cancer Institute grant CA-87567 (to M.H.S.), National Institutes of

Health grant GM-42455 (to S.L.S.), and U.S. Public Health Service grants GM-47214 and HL-57900 (to M.A.S.).

## REFERENCES

- Altschuler, Y., Barbas, S.M., Terlecky, L.J., Tang, K., Hardy, S., Mostov, K.E., and Schmid, S.L. (1998). Redundant and distinct functions for dynamin-1 and dynamin-2 isoforms. *J. Cell Biol.* *143*, 1871–1881.
- Baldassarre, M., Pompeo, A., Castaldi, C., Cortelino, S., Beznoussenko, G., McNiven, M. A., Luini, A., and Buccione, R. (2003). Dynamin participates in focal extracellular matrix degradation by invasive cells. *Mol. Biol. Cell* *14*, 1074–1083.
- Benard, V., Bohl, B.P., and Bokoch, G.M. (1999). Characterization of rac and cdc42 activation in chemoattractant-stimulated human neutrophils using a novel assay for active GTPases. *J. Biol. Chem.* *274*, 13198–13204.
- Bray, D., and White, J.G. (1988). Cortical flow in animal cells. *Science* *239*, 883–888.
- Cao, H., Garcia, F., and McNiven, M.A. (1998). Differential distribution of dynamin isoforms in mammalian cells. *Mol. Biol. Cell* *9*, 2595–2609.
- Ceresa, B.P., and Schmid, S.L. (2000). Regulation of signal transduction by endocytosis. *Curr. Opin. Cell Biol.* *12*, 204–210.
- Damke, H., Baba, T., Warnock, D.E., and Schmid, S.L. (1994). Induction of mutant dynamin specifically blocks endocytic coated vesicle formation. *J. Cell Biol.* *127*, 915–934.
- Damke, H., Baba, T., van der Bliek AM., Schmid SL. (1995). Clathrin-independent pinocytosis is induced in cells overexpressing a temperature-sensitive mutant of dynamin. *J. Cell Biol.* *131*, 69–80.
- Damke, H., Binns, D.D., Ueda, H., Schmid, S.L., and Baba, T. (2001). Dynamin GTPase domain mutants block endocytic vesicle formation at morphologically distinct stages. *Mol. Biol. Cell*, *12*, 2578–2589.
- Del Pozo, M.A., Kiesses, W.B., Alderson, N.B., Meller, N., Hahn, K.M., and Schwartz, M.A. (2002). Integrins regulate GTP-Rac localized effector interactions through dissociation of Rho-GDI. *Nat. Cell Biol.* *4*, 232–239.
- del Pozo, M.A., Price, L.S., Alderson, N.B., Ren, X.D., and Schwartz, M.A. (2000). Adhesion to the extracellular matrix regulates the coupling of the small GTPase Rac to its effector PAK. *EMBO J.* *19*, 2008–2014.
- Di Fiore, P.P., and De Camilli, P. (2001). Endocytosis and signaling: an inseparable partnership. *Cell* *106*, 1–4.
- Dharmawardhane, S., Schurmann, A., Sells, M.A., Chernoff, J., Schmid, S.L., and Bokoch, G.M. (2000). Regulation of macropinocytosis by p21-activated kinase-1. *Mol. Biol. Cell* *11*, 3341–3352.
- Fish, K.N., Schmid, S.L., and Damke, H. (2000). Evidence that dynamin-2 functions as a signal-transducing GTPase. *J. Cell Biol.* *150*, 145–154.
- Gold, E.S., Underhill, D.M., Morrissette, N.S., Guo, J., McNiven, M.A., and Aderem, A. (1999). Dynamin 2 is required for phagocytosis in macrophages. *J. Exp. Med.* *190*, 1849–1856.
- Hawkins, P.T., *et al.* (1995). PDGF stimulates an increase in GTP-Rac via activation of phosphoinositide 3-kinase. *Curr. Biol.* *5*, 393–403.
- Henley, J.R., Krueger, E.W., Oswald, B.J., and McNiven, M.A. (1998). Dynamin-mediated internalization of caveolae. *J. Cell Biol.* *141*, 85–99.
- Hislop, J.N., Everest, H.M., Flynn, A., Harding, T., Uney, J.B., Troskie, B.E., Millar, R.P., and McArdle, C.A. (2001). Differential Internalization of mammalian and non-mammalian gonadotropin-releasing hormone receptors. *J. Biol. Chem.* *276*, 39685–39694.
- Kranenburg, O., Verlaan, I., and Moolenaar, W.H. (1999). Dynamin is required for the activation of mitogen-activated protein kinase by MAP kinase kinase. *J. Biol. Chem.* *274*, 35301–35304.
- Kraynov, V.S., Chamberlain, C., Bokoch, G.M., Schwartz, M.A., Slabaugh, S., and Hahn, K.M. (2000). Localized rac activation dynamics visualized in living cells. *Science* *290*, 333–337.
- Krueger, E.W., Orth, J.D., Cao, H., and McNiven, M. (2003). A dynamin-cortactin-Arp2/3 complex mediates actin reorganization in growth factor-stimulated cells. *Mol. Biol. Cell* *14*, 1085–1096.
- Lamaze, C., Dujeancourt, A., Baba, T., Lo, C.G., Benmerah, A., and Dautry-Varsat, A. (2001). Interleukin 2 receptors and detergent-resistant membrane domains define a clathrin-independent endocytic pathway. *Mol. Cell* *7*, 661–671.
- Lee, E., and De Camilli, P. (2002). Dynamin at actin tails. *Proc. Natl. Acad. Sci. USA* *99*, 161–166.

- McNiven, M.A., Cao, H., Pitts, K.R., and Yoon, Y. (2000a). The dynamin family of mechanoenzymes: pinching in new places. *Trends Biochem. Sci.* *25*, 115–120.
- McNiven, M.A., Kim, L., Krueger, E.W., Orth, J.D., Cao, H., and Wong, T.W. (2000b). Regulated interactions between dynamin and the actin-binding protein cortactin modulate cell shape. *J. Cell Biol.* *151*, 187–198.
- Ochoa, G.C., *et al.* (2000). A functional link between dynamin and the actin cytoskeleton at podosomes. *J. Cell Biol.* *150*, 377–389.
- Oh, P., McIntosh, D.P., and Schnitzer, J.E. (1998). Dynamin at the neck of caveolae mediates their budding to form transport vesicles by GTP-driven fission from the plasma membrane of endothelium. *J. Cell Biol.* *141*, 101–114.
- Orth, J.D., Krueger, E.W., Cao, H., and McNiven, M.A. (2002). The large GTPase dynamin regulates actin comet formation and movement in living cells. *Proc. Natl. Acad. Sci. USA* *99*, 167–172.
- Orth, J.D., and McNiven, M.A. (2003). Dynamin at the actin-membrane interface. *Curr. Opin. Cell Biol.* *15*, 31–39.
- Pelkmans, L., Puntener, D., and Helenius, A. (2002). Local actin polymerization and dynamin recruitment in SV40-induced internalization of caveolae. *Science* *296*, 535–539.
- Price, L.S., Leng, J., Schwartz, M.A., and Bokoch, G.M. (1998). Activation of Rac and Cdc42 by integrins mediates cell spreading. *Mol. Biol. Cell* *9*, 1863–1871.
- Radhakrishna, H., Al-Awar, O., Khachikian, Z., and Donaldson, J.G. (1999). ARF6 requirement for Rac ruffling suggests a role for membrane trafficking in cortical actin rearrangements. *J. Cell Sci.* *112*, 855–866.
- Ridley, A.J., Paterson, H.F., Johnston, C.L., Diekmann, D., and Hall, A. (1992). The small GTP-binding protein rac regulates growth factor-induced membrane ruffling. *Cell* *70*, 401–410.
- Salmon, W.C., Adams, M.C., and Waterman-Storer, C.M. (2002). Dual-wavelength fluorescent speckle microscopy reveals coupling of microtubule and actin movements in migrating cells. *J. Cell Biol.* *158*, 31–37.
- Sander, E.E., ten Klooster, J.P., van Delft, S., van der Kammen, R.A., and Collard, J.G. (1999). Rac downregulates Rho activity: reciprocal balance between both GTPases determines cellular morphology and migratory behavior. *J. Cell Biol.* *147*, 1009–1022.
- Schafer, D.A., Weed, S.A., Binns, D., Karginov, A.V., Parsons, J.T., and Cooper, J.A. (2002). Dynamin2 and cortactin regulate actin assembly and filament organization. *Curr. Biol.* *12*, 1852–1857.
- Schmid, S.L., McNiven, M.A., and De Camilli, P. (1998). Dynamin and its partners: a progress report. *Curr. Opin. Cell Biol.* *10*, 504–512.
- Small, J.V., Stradal, T., Vignall, E., and Rottner, K. (2002). The lamellipodium: where motility begins. *Trends Cell Biol.* *12*, 112–120.
- Swanson, J.A. (1989). Phorbol esters stimulate macropinocytosis and solute flow through macrophages. *J. Cell Sci.* *94*, 135–142.
- Swanson, J.A., and Watts, C. (1995). Macropinocytosis. *Trends Cell Biol.* *5*, 424–428.
- van der Blik, A.M., Redelmeier, T.E., Damke, H., Tisdale, E.J., Meyerowitz, E.M., and Schmid, S.L. (1993). Mutations in human dynamin block an intermediate stage in coated vesicle formation. *J. Cell Biol.* *122*, 553–563.
- Warnock, D.E., Terlecky, L.J., and Schmid, S.L. (1995). Dynamin GTPase is stimulated by crosslinking through the C-terminal proline-rich domain. *EMBO J.* *14*, 1322–1328.